Desalination and Water Treatment
www.deswater.com

doi: 10.5004/dwt.2019.23790

150 (2019) 396–405
May

Comparative evaluation of alkali precipitation and electrodeposition for copper removal in artisanal gold smelting wastewater in the Philippines

Eleazer L. Vivas[a,b,c,*], Catalino G. Alfafara[a], Veronica P. Migo[a], Kuk Cho[b], Monet Concepcion M. Detras[a], Lorele C. Trinidad[d], Marlo D. Mendoza[e], Sumin Lee[b]

[a]*Department of Chemical Engineering, College of Engineering and Agro-Industrial Technology, University of the Philippines Los Baños, College 4031, Laguna, Philippines, Tel. +63495362315; emails: linojp@yahoo.com (C.G. Alfafara), vpmigo@up.edu.ph (V.P. Migo), mmdetras@up.edu.ph (M.C.M. Detras)*
[b]*Laboratory of Particle and Sustainable Technology, Department of Environmental Engineering, College of Engineering, Pusan National University, 2 Busandaehak-ro 63beon-gil, Geumjeong-gu, Busan 46241, South Korea, Tel. +82515102418; emails: eleazer.vivas@gmail.com, elvivas@pusan.ac.kr (E.L.Vivas), kukcho@pusan.ac.kr, kukcho73@gmail.com (K. Cho), leesmmm@pusan.ac.kr, leesu3614@gmail.com (S. Lee)*
[c]*College of Arts and Sciences, Batangas State University, JPLPC–Malvar Campus, Gov. Leviste St., Poblacion, Malvar 4233, Batangas, Philippines, Tel. +63434060830; ext. 122*
[d]*National Institute of Molecular Biology and Biotechnology, University of the Philippines Los Baños, College 4031, Laguna, Philippines, Tel. +63495360587; email: lctrinidad@up.edu.ph*
[e]*Social Forestry and Forest Governance, College of Forestry and Natural Resources, University of the Philippines Los Baños, College 4031, Laguna, Philippines, Tel. +63495363493; emails: mdmendoza2@up.edu.ph, marlobk@gmail.com*

Received 16 August 2018; Accepted 10 January 2019

ABSTRACT

Alkali precipitation and electrodeposition for copper removal in artisanal gold smelting wastewater were evaluated. Alkali precipitation was done by dosing the wastewater with sodium hydroxide solution. Electrodeposition was conducted at operating current of 4 A for 3 and 6 h. Alkali treatment exhibited 99.83% removal efficiency, albeit residual copper concentration was still above effluent standards. Lead was no longer detected at pH ≥ 6 while 87.82% of cadmium was removed at maximum precipitation. Generation of metal hydroxide sludge implied the need for a post-treatment. Electrodeposition demonstrated superior copper removal efficiency (99.98%). With appropriate selection of electrolysis time, it could achieve complete copper removal. It had low energy consumption and indicative treatment cost, and no sludge generation. Electrodeposition current efficiency was relatively low due to other wastewater components which could have consumed a fraction of applied current. Kinetics evaluation showed a three-step electrodeposition process, each stage having a different reaction rate order. Lead was not detected after 3 h while 50.00% of cadmium was removed after 6-h electrolysis. Considering removal efficiency without sludge generation, indicative treatment cost, and value recovery of deposited copper, results revealed that electrodeposition has some advantage over alkali precipitation for the remediation of artisanal gold smelting wastewater.

Keywords: Artisanal gold smelting; Chemical precipitation; Copper removal; Current efficiency; Electrochemical treatment; Electrodeposition; Heavy metals

---

[*] Corresponding author.

1. Introduction

The province of Bulacan in Central Luzon, Philippines houses the Marilao-Meycauyan-Obando river system (MMORS) which is a major hub for aquaculture. MMORS supplies water to thousands of hectares of commercial fishponds, making Bulacan one of the top producers of milkfish and tilapia in the Philippines [1,2]. However, Pure Earth (then Blacksmith Institute), a New York-based not-for-profit organization, included MMORS in their Dirty 30 list of the world's worst polluted places in 2007 due to hazardous wastes the river system receives from tanneries, artisanal gold, precious metal refineries, lead acid battery recycling and smelting plants, and backyard pyrotechnics [3,4]. Wastewaters from these industries usually contain heavy metal ions which are toxic, non-biodegradable, and easily bioaccumulated thus adversely affecting the environment and human health [5–10]. Among heavy metals, copper is commonly present at high levels in wastewater as it is usually employed in electroplating, electronics, metal finishing, etching, and other industrial applications [11–14]. Analysis of water samples from MMORS revealed high dissolved copper concentrations that exceeded both local and international effluent standards [15,16]. The effluents from unregulated artisanal gold smelting operations along the stretch of the river system are the identified culprit of copper contamination.

Unlike traditional gold smelting which extracts gold from its ores, artisanal gold smelting within the MMORS region is a process of recovering high-purity gold from old used jewelry, scrap printed circuit boards, and other gold concentrates. The process is quite simple because many Bulacan households are engaged in it [17]. A schematic diagram of a typical artisanal gold smelting process, which is based on an actual visit to a small-scale refinery in Meycauayan, Bulacan, is presented in Fig. 1. The process begins with old jewelry and silver heated to their molten states. Gold migrates to the molten silver, forming a melt bilayer of silver-gold amalgam and metal impurities. The amalgam is separated from the impurities then quenched with fuming nitric acid and water to oxidize silver as silver nitrate. The nitric acid-insoluble gold is collected then heated to high-purity gold. The silver-rich acidic effluent undergoes displacement reaction with copper bars to recover silver for reuse in the initial step. The silver recovery process generates a copper-rich acidic wastewater which is non-compliant to the Philippine Department of Environment and Natural Resources (DENR) permissible limit of 0.04 mg L^{-1} dissolved copper for Class C water (i.e. waters used for fisheries, recreational boating, and industrial cooling) [18] and to the U.S. Environmental Protection Agency (EPA) threshold copper concentration of 3.38 mg L^{-1} for electroplating and metal finishing effluents [19]. The artisanal gold smelting wastewater also contains traces of lead and cadmium as these are inherent impurities in jewelry.

Discharge of unregulated copper-rich artisanal gold smelting effluents is detrimental to aquatic environments especially to fish farms downstream the MMORS. Soil, riverbed/sediments, plants, and animals are prone to copper exposure. Eventually, dissolved copper will find its way into the food chain and drinking water, contaminating residents near the river system. The people of Bulacan are also susceptible to direct contamination as low-lying areas are inundated with polluted waters of MMORS during high tides and extreme inclement weather conditions. Exposure to copper has adverse effects on human health, such as anemia, liver and kidney damage, stomach and intestinal distress, and hair loss [20–22]. Therefore, careful treatment of artisanal gold smelting wastewater is necessary to comply with effluent standards and preclude the ferocity of copper contamination in the environment and public health.

Registered artisanal gold refiners within the MMORS region employ alkali precipitation with caustic soda as the precipitating agent as shown in Fig. 1. Alkali precipitation is one of the conventional treatment technologies which most industries prefer as the first treatment option because of its relatively lower cost. However, it is often applied based on theoretical solubilities which may not be reliable during actual treatment, and it generates metal hydroxide sludge, a secondary waste. Emerging and advanced techniques

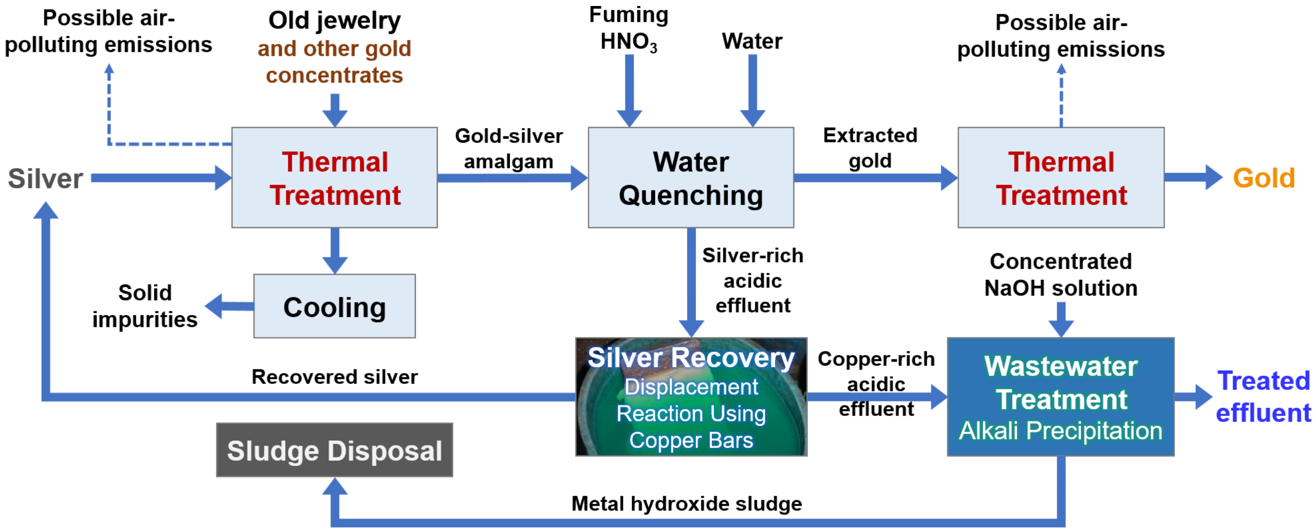

Fig. 1. Schematic of a typical artisanal gold smelting process in Bulacan, Philippines.

have been employed for the removal of copper from industrial wastewaters, such as adsorption [7,12,14,20–22], ion flocculation [13], ion exchange [23,24], photocatalysis [25–27], and forward osmosis [28,29]. These are effective but not yet practical for field application in terms of cost effectiveness and considering the technological preparedness of the end users. Most of the available conventional treatment systems, on the other hand, are based on physical displacement or chemical replacement, generating yet another problem in the form of toxic sludge, the disposal of which adds further burden on the techno-economic feasibility of the treatment process. Pursuit of more cost-effective processes for toxic heavy metal-contaminated wastewaters has directed attention to electrodeposition which can remove Cu^{2+} ions from an aqueous solution and reduce them into metallic copper deposits onto an insoluble electrode. Electrodeposition had demonstrated high copper removal in actual and simulated industrial effluents or wastes [11,30–33] but not much literature highlighted its application in treating artisanal gold smelting wastewater. Regarded as a clean technology, electrodeposition has the following major advantages over conventional treatment methods: (1) high efficiency, (2) environmentally benign (i.e. minimization of toxic chemical and biological sludge), (3) technologically available, and (4) potential commercial value of recovered metal which could offset any increase in energy cost [11,30–34].

To provide artisanal gold smelting firms information in selecting the treatment option they would want to use for satisfactorily treating their effluents thus contributing to the ongoing clean-up operations and intensified revival programs for the MMORS by government and non-government units, this research investigated the performance of alkali precipitation and electrodeposition in removing copper from actual gold smelting wastewater. Not much literature had reported comparative treatment evaluation for actual artisanal gold smelting wastewater per the aforementioned purpose. In alkali precipitation, several alkali doses were tested to reach certain pH conditions and obtain an actual precipitation curve. Copper removal efficiency, optimum alkali dose and pH for maximum precipitation, and metal hydroxide sludge production were evaluated. In electrodeposition, the wastewater was electrolyzed at constant operating current to come up with residual copper profiles. Metal removal efficiencies and final copper concentrations, charge dose, current efficiency, and copper electrodeposition kinetics were assessed. Removal efficiencies for lead and cadmium were also evaluated in both processes. Finally, a comparison of indicative treatment costs was made. This study did not attempt to determine, control, and evaluate the presence of other pollutants in the wastewater.

2. Materials and methods

All experiments were conducted at an isolated room where temperature was kept at about 30°C to simulate normal environmental condition.

2.1. Preparation and characterization of wastewater

Two carboys full of artisanal gold smelting wastewater were obtained from a small-scale artisanal gold smelting plant in Meycauayan, Bulacan, Philippines. It was then transported and stored at room temperature in an analytical chemistry laboratory. The wastewater was characterized in terms of pH, heavy metals content (i.e. copper, lead, and cadmium), and conductivity. It was subjected to alkali precipitation and electrodeposition experiments without any purification or dilution.

Conductivity of the actual wastewater was measured using a benchtop conductivity meter (Horiba D-24 pH/conductivity meter, Japan).

2.2. Alkali precipitation experiment

The precipitation reactor was a modified rubber cap-sealed 1-L Erlenmeyer flask with a working volume of 620 mL. Electrode of an Orion pH meter (Expandable Ion Analyzer EA 940) was immersed in the wastewater for continuous pH monitoring. By carefully adding 50% w/v sodium hydroxide (NaOH pellets, >98%, SAMCHUN, South Korea) solution to the wastewater, pH values 2, 4, 6, 9 and 12 were reached. The wastewater was sparged with N_2 gas (99.9995%, Linde Group–Philippines) to purge CO_2, which may affect pH readings, in the reactor's headspace while continuously agitated by a magnetic stirrer (Fischer Scientific Thermix 620T, U.S.) at 600 rpm. Sampling was done after achieving each target pH. Filtered (using Whatman GF/C filter paper, 110 mm diam.) and unfiltered liquid samples were prepared for analyses. Actual precipitation reactor is illustrated in Fig. 2(a).

2.3. Batch electrodeposition experiment

A 1-L glass beaker with a working volume of 750 mL was used as an open-air batch reactor for the electrodeposition of gold smelting wastewater. The electrode package used is composed of 50 × 150 mm (width × length) stainless steel (cathode) and sintered platinum (anode) plates with a rubber spacing of about 5 mm. The electrodes were generously donated by Prof. Masatoshi Matsumura of the Institute of Applied Biochemistry, University of Tsukuba, Japan. The operating current was supplied by a direct current regulated power generator (GSV 3000, Diamond Co., Tokyo, Japan). A round clamp ammeter (Wheeler HD-3311 clamp meter, Taiwan) connected to a multimeter (Newstar DT-830b digital multimeter, China) was used to monitor constant current of 4 A. Batch electrodeposition runs were performed for 3 and 6 h with continuous stirring at 400 rpm. Sampling per each run was done periodically. Temperature and pH of the wastewater were monitored. Actual electrodeposition setup is shown in Fig. 2(b).

2.4. Analyses

Metal ion concentrations of liquid samples were determined using an atomic absorption spectrophotometer (Perkin-Elmer AAnalyst 200, U.S.). Cu removal efficiencies were calculated using Eq. (1).

$$\text{Removal efficiency} = \left(1 - \frac{C_o}{C_t}\right) \times 100 \tag{1}$$

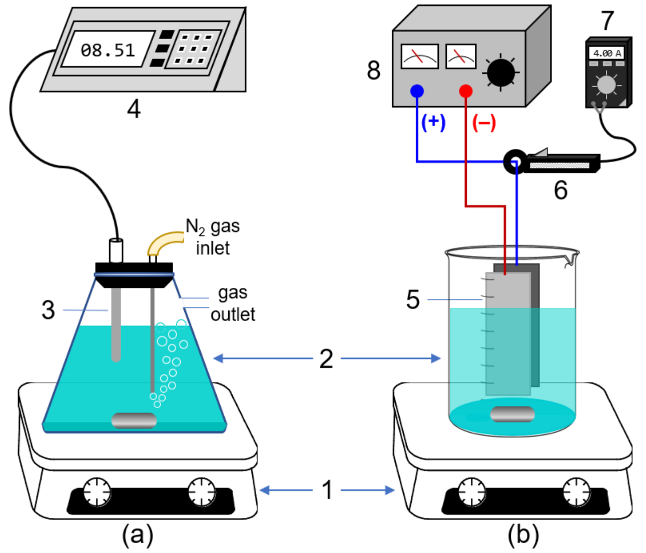

Fig. 2. Illustrations of the batch (a) alkali precipitation and (b) electrodeposition lab setups: 1 – magnetic stirrers, 2 – (a) and (b) batch reactors, 3 – pH probe, 4 – pH meter, 5 – electrode package, 6 – round clamp ammeter, 7 – multimeter, and 8 – DC regulated power generator.

Alkali dose, which is simply the amount of precipitant in grams per unit volume of wastewater needed to reach a certain pH, was calculated according to Eq. (2).

$$\text{Alkali dose} = \frac{V_p \times C_p}{V_w} \tag{2}$$

Precipitation sludge production as total suspended solids (TSS) was gravimetrically estimated using Eq. (3). Whatman Glass Microfibre Filters (934-AH, 47 mm diameter) were used in TSS determination.

$$\text{TSS} = \frac{w_1 - w_o}{V_w} \tag{3}$$

Charge dose (*Q*), a scale-up parameter for electrolytic reactors, was measured using Eq. (4). It is defined as the amount of charge required to remove a unit mass of target pollutant.

$$Q = \frac{It}{\left(C_o - C_t\right)V_w} \tag{4}$$

Current efficiency (φ) of the electrodeposition process was calculated using Eq. (5) [34].

$$\varphi = \frac{wnF}{IMt} \tag{5}$$

Cathode deposits for the 3-h and 6-h electrodeposition runs were gravimetrically measured by simply taking the difference of the dry weights of the electrode package before and after electrodeposition. A digital top loading balance (BALANCE 5 TX2202L, Shimadzu, Japan) was used to determine the weights.

Kinetics of copper electrodeposition in artisanal gold smelting wastewater was evaluated using pseudo zero-, pseudo first-, and pseudo second-order equations expressed in Eqs. (6)–(8).

$$C_t = C_o - k_o t \tag{6}$$

$$\ln\left(C_t\right) = \ln\left(C_o\right) - k_1 t \tag{7}$$

$$\frac{1}{C_t} = k_2 t + \frac{1}{C_o} \tag{8}$$

2.5. Comparison of indicative treatment costs

Indicative treatment costs were derived from the results of the alkali precipitation and electrodeposition experiments to further recommend the better treatment method for gold smelting wastewater. Indicative material cost for precipitation per unit volume of wastewater was computed by multiplying optimum alkali dose with the local market price of technical grade NaOH of 110 PhP kg^{-1} (2.2 US\$ kg^{-1}) [35,36]. On the other hand, the energy requirement (kWh mg^{-1} copper) for electrodeposition was estimated using Eq. (9). Indicative electrodeposition cost was estimated by getting the product of energy requirement and the average local electricity cost of 10.32 PhP kWh^{-1} (0.2064 US\$ kWh^{-1}) [36,37].

$$\text{Energy requirement} = 3.6 \times 10^{-6}\left(\text{Q} \times \text{E}\right) \tag{9}$$

3. Results and discussion

3.1. Gold smelting wastewater characteristics

The actual gold smelting wastewater had copper, lead, and cadmium contents of 8,752.62, 7.14, and 1.15 mg L^{-1}, respectively. It was extremely acidic (pH < 1) and demonstrated high conductivity of 114.8 mS cm^{-1}. The blue color of the wastewater indicated high dissolved Cu^{2+} ions. In an interview with the operation head of the medium-scale artisanal gold smelting industry, Cu^{2+} was the cation with the highest concentration in their effluent since copper bars were being used to recover silver in their gold smelting process (silver recovery stage, Fig. 1). Moreover, trace amounts of copper were already present in processed old jewelry along with lead and cadmium as inherent impurities.

3.2. Cu removal efficiency of alkali precipitation

The main objective of alkali precipitation for practical application is to determine the optimum pH for maximum removal of metal ion as metal hydroxide. The solubility curve relating pH with Cu^{2+} concentration in the actual wastewater was investigated. An actual alkali precipitation is more reliable in evaluating the optimum pH compared with the theoretical precipitation curve because all other interacting factors (i.e. presence of other solutes) are accounted for. Fig. 3 shows the residual metal ion concentrations, the removal efficiencies, and visual observations for the effluent during precipitation at different pH values.

Clear and distinct changes in color, degree of turbidity, and amount of precipitates formed were observed as pH was increased. Turbidity increased at higher pH values due to higher precipitation of the metal hydroxide. The filtrate of the liquid samples at pH 6, 9, and 12 were visibly clear and colorless, indicating considerable copper removals. The lowest possible dissolved concentration of copper based on the theoretical solubility of $Cu(OH)_2$ was approximately 0.001 mg L^{-1} at pH 8.1 [38,39]. The lowest value of copper solubility was 15.06 mg L^{-1} at pH values equal to or greater than 6 as presented in the actual precipitation curve (Fig. 3). The different pH-concentration relationship between the precipitation of $Cu(OH)_2$ in actual wastewater and that in pure water was attributed to other unknown dissolved metals and components present in the actual wastewater which affected $Cu(OH)_2$ solubility. It should be noted that removal of metals from mixed-metal wastes may not be effective because the minimum solubilities for different metals occur at different pH conditions. Furthermore, the wastewater might have complexing agents which adversely affected metal removal. Although alkali precipitation demonstrated 99.83% copper removal, the residual Cu^{2+} at pH 6 or greater did not comply with the effluent standards.

The precipitation behavior of Pb^{2+} and Cd^{2+} in their hydroxide forms was also investigated and data obtained were compared with their respective theoretical solubilities. Like the case of Cu^{2+}, the actual solubilities of Pb^{2+} and Cd^{2+} in Fig. 3 were different from their respective theoretical solubilities. The theoretical pH values for maximum precipitation of Pb^{2+} and Cd^{2+} were 8.8 and 10.5, respectively [38,39]. The corresponding values from the actual precipitation curves were pH 6 and pH 12 for Pb^{2+} and Cd^{2+}, respectively. Pb^{2+} ions were no longer detected by AAS at pH 6, indicating its complete removal as $Pb(OH)_2$ while residual Cd^{2+} concentration at maximum precipitation (pH 12) was 0.14 mg L^{-1} which was commensurate to 87.82% Cd removal. The differences in actual precipitation and theoretical solubilities were attributed to the presence of other components in the artisanal gold smelting wastewater which may have affected their solubilities. Residual Cd^{2+} concentrations at pH values greater than or equal to 6 did not comply with the US EPA and DENR effluent standards.

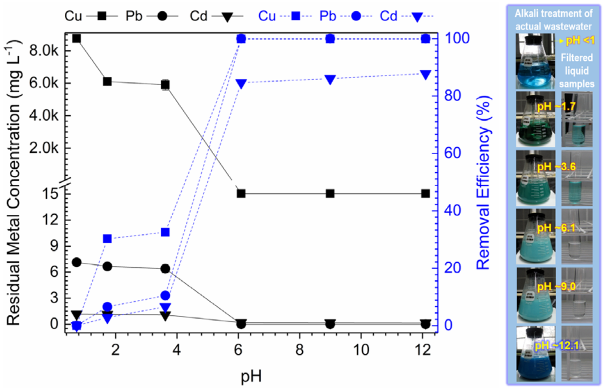

Fig. 3. Performance of alkali precipitation in the removal of copper, lead and cadmium, and optical images during actual treatment of artisanal gold smelting wastewater.

3.3. Alkali dose and metal hydroxide sludge production

Fig. 4 shows that alkali dose increased as the pH for precipitation increased. The relationship was approximately linear (r^2 = 0.922). Optimum pH for the precipitation of Cu^{2+} was 6 which was achieved upon addition of 12.99 g NaOH per liter of the wastewater. The same alkali dose was needed for the maximum precipitation of Pb^{2+} and Cd^{2+} as metal hydroxides with compliance to effluent standards for pH (6–9). Table 1 shows that the amount of sludge produced was 18.0 g L^{-1} wastewater, about 5 units greater than the theoretical sludge production based on residual metal ion concentration analysis. This implied that other metals (e.g. unrecovered silver, gold) were present in the wastewater.

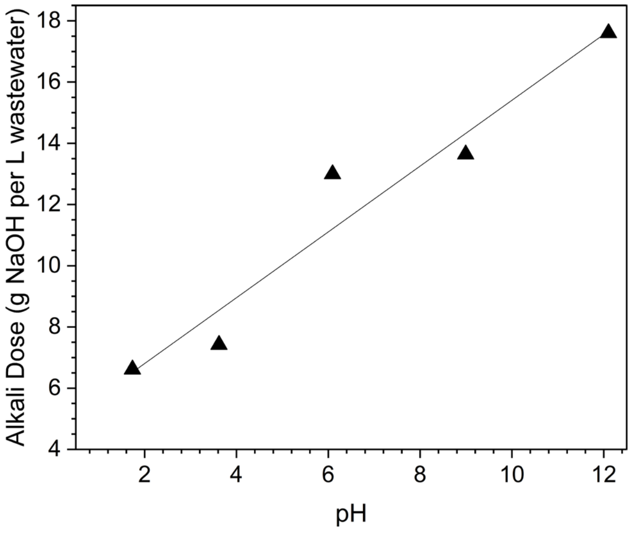

Fig. 4. Linearized alkali dose plot for the treatment of artisanal gold smelting wastewater using 50% w/v NaOH solution.

Table 1
Theoretical and actual amounts of precipitation sludge at pH values per effluent standards

pH values		Metal hydroxide sludge produced (g L^{-1})	
Target	Actual	Theoretical[a]	Actual
6.0	6.1	13.42	18.02
9.0	9.0	13.42	18.04
12.0	12.1	13.42	18.04

[a] Based on metal ion analysis of liquid samples through AAS

3.4. Cu removal performance of electrodeposition

Preliminary electrolysis runs were conducted at 2, 4, and 6 A. Electrodeposition at 2 A was very slow that visible deposition started after almost an hour of treatment. At 6 A, metal deposition was very rapid that wastewater became colorless in less than 2 h, and vigorous generation of strong hypochlorite-smelling vapor was observed. Considering more manageable investigation of the electrodeposition process without compromising health and safety concerns due to generation of hazardous vapors, the operating current was fixed at 4 A. To examine the effect of treatment time on the electrodeposition of copper at constant current, 3 and 6-h batch electrolyses were performed.

Fig. 5(c) shows visible color change in the wastewater after electrolytic treatment. The color of the wastewater was altered from blue to a clear, transparent solution, and no precipitate was visible after electrodeposition. Other than color, the evident change was observed on the stainless steel cathode. Reddish brown metal coating around the cathode was seen after the electrolytic treatment. This metal coating could be copper deposits per the electroreduction of Cu^{2+} ions expressed in Eq. (10). The simultaneous electroreduction of water represented by Eq. (11) may have occurred too as gas microbubbles were generated at the cathode during electrolysis. Microbubbles formation was also spotted on the sintered platinum anode. This was more likely the anodic oxidation of water to oxygen gas expressed by chemical Eq. (12). Other than the simultaneous electroreduction of Cu^{2+} and electrolysis of water, evolution of gas with hypochlorite smell was also observed. Although, further experimental identification was necessary, the hypochlorite smell indicated that the wastewater may have had chloride ions which were oxidized into dissolved chlorine gas at the anode then converted to hypochlorite upon reaction with water according to Eqs. (13)–(15).

$$Cu^{2+} + 2e^- \rightarrow Cu_{(s)} \tag{10}$$

$$2H_2O + 2e^- \rightarrow H_2 + 2OH^- \tag{11}$$

$$2H_2O \rightarrow O_2 + 4e^- + 4H^+ \tag{12}$$

$$2Cl^- \rightarrow Cl_2 + 2e^- \tag{13}$$

$$Cl_2 + H_2O \rightarrow HOCl + HCl \tag{14}$$

$$HOCl \leftrightarrow OCl^- + H^+ \tag{15}$$

Figs. 5(a) and (b) show that Cu^{2+} concentration decreased while copper removal efficiency increased with electrolysis time. After 3-h electrolysis, removal efficiency of 99.50% with 44.16 mg L^{-1} dissolved copper was achieved. Copper removal efficiency of 99.98% was attained with final Cu^{2+} concentration of 1.33 mg L^{-1} after 6-h electrolysis. The final dissolved copper level after 6-h electrolysis passed the U.S. EPA guideline but not the DENR effluent standard, though it was much closer to passing compared with the final dissolved copper after 3-h electrolysis and after alkali treatment at pH 6 to 9. Hence, an effluent with a Cu^{2+} concentration complying with both the international and local standards was possible with the right selection of electrolysis time at constant operating current and by increasing the effective electrode area [40–42].

Electrolytic removal of Pb^{2+} and Cd^{2+} was also investigated. Figs. 5(a) and (b) depict that electroreduction of Pb^{2+} and Cd^{2+}, expressed in Eqs. (16) and (17), occurred after an hour and simultaneously with the electrodeposition of copper but at a lower rate, respectively. Copper has a higher redox potential than lead and cadmium [43], hence its electrodeposition was electrochemically favored. Lead was no longer detected after electrolysis which suggested complete removal after 3 h of treatment. Final dissolved cadmium levels and removal efficiencies after 3 and 6-h

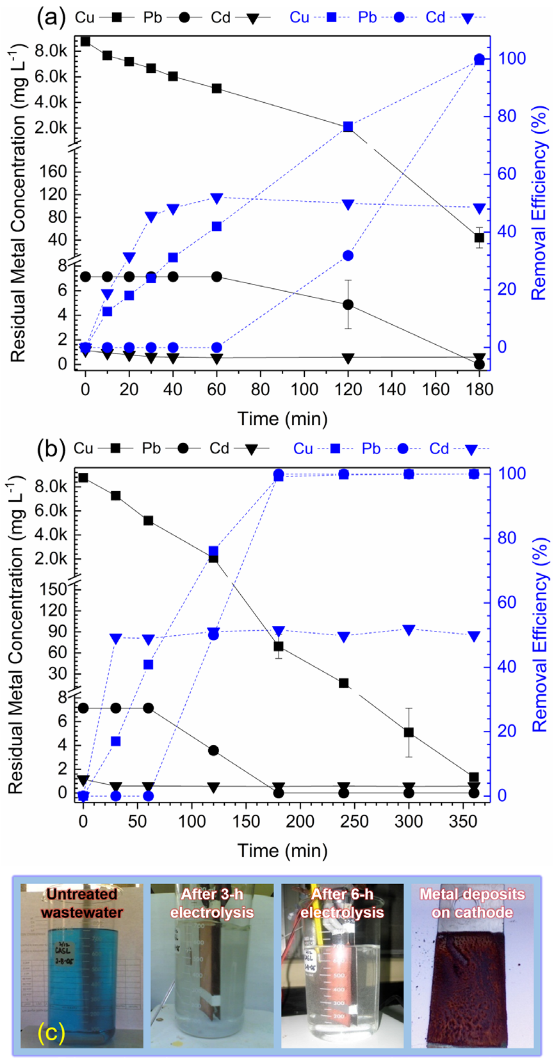

Fig. 5. Performance of (a) 3-h and (b) 6-h electrolyses in the removal of copper, lead, and cadmium from artisanal gold smelting wastewater, and (c) optical images before and after electrolysis.

electrolyses were 0.59 mg L^{-1} and 48.57%, and 0.57 mg L^{-1} and 50.00%, respectively. Electrolyzed wastewater did not pass the effluent standards for cadmium.

$$Pb^{2+} + 2e^- \rightarrow Pb_{(s)} \tag{16}$$

$$Cd^{2+} + 2e^- \rightarrow Cd_{(s)} \tag{17}$$

Table 2 summarizes the amount of metal deposit on the cathode. The weight of cathode deposit after 3-h treatment was equal to the actual copper removed from the wastewater. However, after 6-h treatment, the total cathode deposit was greater than the actual copper removed from the treated wastewater, indicating that other metals could have co-electrodeposited on the cathode after 3 h. This was exemplified by the time courses for Pb^{2+} (Fig. 5) which showed considerable removal at the latter part of electrolysis.

Temperature and pH were monitored during electrodeposition. Fig. 6 shows that temperature increased slightly owing to the heat generated by the resistances of the electrodes, connectors, and the electrolyte. On the other hand, minimal change in pH of the electrolyte during electrodeposition was observed. The mean pH value was near 1, which was very acidic. Although, electroreduction of water (Eq. (11)) may have occurred at the cathode to form OH^- ions which tend to increase pH, the amount may be too small to effect a significant change in the wastewater's extremely acidic nature or may have been offset by the H^+ ions generated through the simultaneous electro oxidation of water (Eq. (12)) at the anode. Also, the wastewater could have unknown buffering components which stabilized the pH. The electrolyzed wastewater's pH should be treated with NaOH or other basic compounds to comply with the effluent standard for pH 6–9.

3.5. Cu deposition charge dose and current efficiency

Fig. 7 shows a linear (r^2 = 0.983) charge dose plot for the electrodeposition process. Charge dose for copper electrodeposition was 6.02 C mg^{-1}. This will be a useful scale-up and operating factor by considering other parameters, such as reactor volume, target copper recovery, operating current, electrode area, and treatment time. On the other hand, current efficiency for copper deposition reached 100.0% during the first 10 min (600 s) of the treatment process and started to decline thereafter until 23.1%, indicating that some of the current were not utilized for copper deposition alone but for other electrode reactions expressed in Eqs. (11)–(17). This suggested that during the early part of electrolysis, applied current for metal deposition was mainly for copper. Looking closely at and comparing Figs. 5 and 7, copper was the major component of the total deposit at the cathode in the first 3 h of electrolysis. As the level of dissolved copper continued to decline, the fraction of the current being consumed for the deposition of copper decreased and operating current was partly utilized by electroreduction of Pb^{2+} and Cd^{2+} ions, and by other electrode reactions thereafter.

Table 2
Actual and theoretical amounts of metal deposition after electrolysis

Electrolysis time (h)	Metal deposits after electrodeposition (g)	
	Theoretical[a]	Actual
3.0	6.54	6.54
6.0	6.57	7.35

[a]Based on metal ion analysis of liquid samples through AAS

3.6. Electrodeposition kinetics

The electrodeposition of copper was found to follow a three-stage process. The kinetics of each phase was correlated to Cu^{2+} concentration. Two transition times (t_1^* = 3,600 s and t_2^* = 14,400 s) were identified. The kinetics of the initial stage of electrodeposition was second-order followed by a shift to zero-order at t_1^* and finally veered to first-order starting at t_2^*. Like many other electrochemical processes, electrodeposition proceeds through a series of reactions characterized by

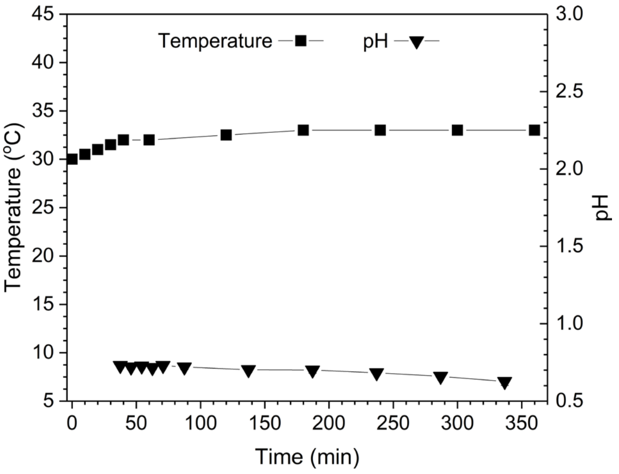

Fig. 6. Temperature and pH profiles during electrodeposition of artisanal gold smelting wastewater.

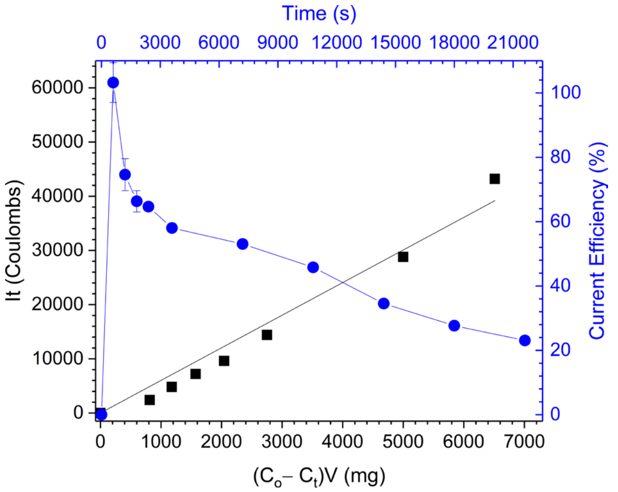

Fig. 7. Charge dose plot and current efficiency profile for the electrodeposition of artisanal gold smelting wastewater at 4 A.

varying kinetic schemes [34,40–42]. The first two steps of electrodeposition were believed to be involved in the electroplating process. Electroplating is a compact deposition process known to have two distinct stages. The first stage involves nuclei formation of the new phase, and its growth to the crystal lattice and formation of thin metal coating on the plating material (i.e. cathode surface). The second stage is plating which involves thickening of the plated layer [34]. The third and final phase of electrodeposition is considered to involve powdery deposition of the remaining dissolved metal in the bulk solution [41,42]. These reaction steps were visually observed during the actual electrolytic treatment of the artisanal gold smelting wastewater. The reddish brown topmost layer of metal deposition on the cathode was powdery as shown in Fig. 5(c). By gently scraping this layer off, a smooth plated layer with red-orange metallic luster was found. The plated layer was easily peeled off from the cathode surface.

At $t \leq t_1^*$, the second-order reaction step is still expressed by Eq. (8). At $t_1^* < t \leq t_2^*$ and $t > t_2^*$, the zero-order and first-order reaction steps are expressed by modified Eqs. (18) and (19), respectively. Table 3 synopsizes the rate constants for the three-step electrodeposition of copper from artisanal gold smelting wastewater.

$$C_{t_1^*} = C_t - k_o\left(t - t_1^*\right) \tag{18}$$

$$\ln\left(C_{t_2^*}\right) = \ln\left(C_t\right) - k_1\left(t - t_2^*\right) \tag{19}$$

3.7. Indicative treatment costs

Material and energy costs per unit volume of wastewater were computed for alkali precipitation and electrodeposition, respectively. These will be useful for artisanal gold smelters in selecting the decontamination option they would employ to satisfactorily treat their effluents based on cost effectiveness. Table 4 compares the indicative cost effectiveness of alkali and electrolytic treatments as well as their level of compliance to effluent standards.

The computed material cost for maximum alkali precipitation at pH 9 was 30.01 US\$ m^{-3} (1,500.38 PhP m^{-3}) wastewater. This would still go up as additional cost is needed for sludge management and disposal. On the other hand, the mean energy requirement for a 6-h electrolysis with an average applied voltage of 3.80 V was 6.35 kWh kg^{-1} copper removed which was translated to an electrical energy cost of 11.47 US\$ m^{-3} (573.64 PhP m^{-3}) wastewater. From the results obtained, the indicative treatment cost of electrodeposition was surprisingly cheaper by about a factor of three compared to that of alkali precipitation. The energy cost could still be minimized by manipulating electrode area and spacing to minimize operating voltage [40–42]. There was no indicative additional cost for sludge disposal because the treatment process did not generate it. The only problem left was the electrolyzed wastewater's extreme acidity which can be solved by conducting a post-treatment in pH adjustment hence an additional cost is required. Nevertheless, the market value of the recovered copper could offset the electrical energy and any post-treatment costs.

Table 3
Rate constants for the electrodeposition of copper from artisanal gold smelting wastewater

Reaction steps	Pseudo zero-order		Pseudo first-order		Pseudo second-order	
	k_o (mol L^{-1} cm^{-2} s^{-1})	r^2	k_1 (cm^{-2} s^{-1})	r^2	k_2 (L s mol^{-1} cm^{-2})	r^2
First	1.69×10^{-5}	0.958	1.48×10^{-4}	0.979	1.30×10^{-3}	0.989
Second	1.10×10^{-5}	0.987	5.99×10^{-4}	0.898	1.30×10^{-1}	0.765
Third	3.41×10^{-8}	0.918	3.53×10^{-4}	0.999	6.11×10^{0}	0.909

Table 4
Comparative evaluation of alkali precipitation and electrodeposition in terms of final metal ion concentrations, pH, and indicative treatment costs at optimum treatment conditions

Treatment and standards	Parameters				
	Final metal conc. (mg L^{-1})			pH	Treatment cost (\$ m^{-3})[a]
	Cu	Pb	Cd		
Alkali precipitation	15.06	n.d.[b]	0.14	9.0	30.01
Electrodeposition	1.33	n.d.	0.57	<1.0	11.47
US EPA standards[c]	3.38	0.69	0.69	6.0–9.0	–
PH DENR standards[d]	0.04	0.10	0.01	6.0–9.0	–

[a] Partial estimate/indicative treatment costs.
[b] No longer detected by Perkin-Elmer AAS.
[c] Guidance manual for electroplating and metal finishing pretreatment/BPT effluent standards.
[d] Class C water – waters used for fisheries, recreational boating, and industrial cooling in the Philippines.

4. Conclusion

This research was able to compare the performance of alkali precipitation and electrodeposition in the removal of copper from artisanal gold smelting wastewater. Results of alkali treatment indicated that using theoretical solubility for extrapolation of precipitation behavior in actual wastewater is not always reliable thus actual experiments should be conducted. A practical single-step alkali precipitation process for copper removal is not sufficient to meet the effluent standards. A second stage treatment as well as the management of metal hydroxide sludge would be necessary. On the other hand, electrodeposition could achieve complete removal of copper with the right selection of electrolysis time for an operating current. However, current efficiency was low as copper is not the only component or pollutant in the actual wastewater. Electrodeposition did not generate sludge. Therefore, the problem in the disposal of toxic sludge, which is common in alkali precipitation and other conventional treatment systems, was circumvented. Electrolyzed artisanal gold smelting wastewater requires final pH adjustment to comply with effluent standards. Thus, a two-step treatment system with copper electrodeposition as the first stage followed by alkali precipitation could be explored. Kinetics evaluation showed that electrodeposition of copper from the wastewater is a three-step process; each step following a different reaction rate order. The indicative cost of electrodeposition treatment is significantly lower than that of alkali precipitation. However, definitive conclusions on the comparative cost could only be made once all cost components are taken into consideration.

Although, some aspects need further investigation, the results obtained from this research point to some advantage of electrodeposition over alkali precipitation (and other available treatment systems) in the removal of copper and other heavy metals from artisanal gold smelting wastewater. The researchers believe that electrodeposition deserves a spot in the list of sustainable treatment options for artisanal gold smelters within the MMORS region to effectively comply with effluent standards; thereby helping the clean-up operations of government and non-government agencies to expedite the revival of MMORS which was once branded as one of the most polluted in the world.

Acknowledgment

This research was supported by the Central Analytical Services Laboratory of the National Institute of Molecular Biology and Biotechnology at the University of the Philippines Los Baños, Basic Science Research Program through the National Research Foundation of Korea (NRF) funded by the Ministry of Education (NRF–2017R1D1A3B03028812), and Brain Korea 21 Plus Project in the Division of Creative Low Impact Development and Management for Ocean Port City Infrastructures (21A20132012304).

Symbols

C_o and C_t – Initial and residual metal concentrations, mg L^{-1}
t – Time, s
C_p – Precipitant concentration, g mL^{-1}
V_p – Precipitant volume, mL
V_w – Volume of treated wastewater, L
TSS – Metal hydroxide sludge as total suspended solids, g L^{-1}
W_0 and W_1 – Initial and final masses of filter papers in TSS determination, g
Q – Charge dose, C mg^{-1}
I – Current, A
ϕ – Current efficiency, %
W – Mass of the metal deposit in electrolysis, g
n – Number of electrons in the balanced electrochemical equation
F – Faraday's constant, 96,485.3329 C mol^{-1}
M – Molecular weight of the metal pollutant, g mol^{-1}
k_0 – Pseudo zero-order electrodeposition rate constant, mol L^{-1} cm^{-2} s^{-1}
k_1 – Pseudo first-order electrodeposition rate constant, cm^{-2} s^{-1}
k_2 – Pseudo second-order electrodeposition rate constant, L s mol^{-1} cm^{-2}
E – Average applied voltage in electrodeposition, V
t_1^* and t_2^* – Transition times in electrodeposition kinetics, s
$C_{t_1^*}$ and $C_{t_2^*}$ – Metal concentrations at transition times in electrodeposition kinetics, mg L^{-1}

References

[1] Pure Earth (Blacksmith Institute), Annual Report 2016. Available at: http://www.pureearth.org/wp-content/uploads/2014/12/PE_AnnualReport.pdf (Accessed 12 June 2018).

[2] Pure Earth (Blacksmith Institute), Annual Report 2015. Available at: http://www.pureearth.org/wp-content/uploads/2014/12/PE_AnnualReportSm.pdf (Accessed 12 June 2018).

[3] N. Espina, Meycauayan, Marilao in World's 'Dirty 30' – report (2007). Available at: http://newsinfo.inquirer.net/breakingnews/regions/view_article.php?article_id=89091 (Accessed 07 May 2018).

[4] Pure Earth (Blacksmith Institute), Annual Report 2008. Available at: http://www.pureearth.org/wp-content/uploads/2014/12/PE_AnnualReportSm.pdf (Accessed 07 May 2018).

[5] A. Asfaram, M. Ghaedi, G.R. Ghezelbash, Biosorption of Zn^{2+}, Ni^{2+} and Co^{2+} from water samples onto Yarrowia lipolytica ISF7 using a response surface methodology and analyzed by inductively coupled plasma optical emission spectrometry (ICP-OES), RSC. Adv., 6 (2016) 23599–23610.

[6] F.R. Peligro, I. Pavlovic, R. Rojas, C. Barriga, Removal of heavy metals from simulated wastewater by in situ formation of layered double oxides, Chem. Eng. J., 306 (2016) 1035–1040.

[7] J.H. Zhao, J. Liu, N. Li, W. Wang, J. Nan, Z.W. Zhao, F.Y. Cui, Highly efficient removal of bivalent heavy metals from aqueous systems by magnetic porous Fe_3O_4–MnO_2: adsorption behavior and process study, Chem. Eng. J., 304 (2017) 737–746.

[8] E.A. Dil, M. Ghaedi, A. Asfaram, S. Hajati, F. Mehrabi, A. Goudarzi, Preparation of nanomaterials for the ultrasound-enhanced removal of Pb^{2+} ions and malachite green dye: chemometric optimization and modeling, Ultrason. Sonochem., 34 (2017) 677–691.

[9] J.A. Conkling, C.J. Mocella, Chemistry of Pyrotechnics: Basic Principles and Theory, 2nd Ed., CRC Press – Taylor & Francis Group, Boca Raton, FL, USA, 2010.

[10] F.N. Azad, M. Ghaedi, K. Dashtian, A. Jamshidi, G. Hassani, M. Montazerozohori, S. Hajati, M. Rajabi, A.A. Bazrafshan,

Preparation and characterization of an AC–Fe_3O_4–Au hybrid for the simultaneous removal of Cd^{2+}, Pb^{2+}, Cr^{3+} and Ni^{2+} ions from aqueous solution via complexation with 2-((2,4-dichlorobenzylidene)-amino)-benzenethiol: taguchi optimization, RSC. Adv., 6 (2016) 19780–19791.

[11] M. Hunsom, K. Pruksathorn, S. Damronglerd, H. Vergnes, P. Duverneuil, Electrochemical treatment of heavy metals (Cu^{2+}, Cr^{6+}, Ni^{2+}) from industrial effluent and modeling copper reduction, Water. Res., 39 (2005) 610–616.

[12] J. Gao, F. Liu, P. Ling, J. Lei, L. Li, C. Li, A. Li, High efficient removal of Cu(II) by a chelating resin from strong acidic solutions: complex formation and DFT certification, Chem. Eng. J., 222 (2013) 240–247.

[13] G.K.G.C. Barros, R.P.F. Melo, E.L.B. Neto, Removal of copper ions using sodium hexadecanoate by ionic flocculation, Sep. Purif. Technol., 200 (2018) 294–299.

[14] N. Moscatello, G. Swayambhu, C.H. Jones, J. Xu, N. Dai, B.A. Pfeifer, Continuous removal of copper, magnesium, and nickel from industrial wastewater utilizing the natural product yersiniabactin immobilized within a packed-bed column, Chem. Eng. J., 343 (2018) 173–179.

[15] Asian Development Bank, Reducing Mercury and Heavy Metals Contamination in Meycauayan River (2009). Available at: https://www.adb.org/results/water-pda-reducing-mercury-and-heavy-metals-contamina tion-meycauayan-river (Accessed 15 June 2018).

[16] Pure Earth (Blacksmith Institute), GAHP, Green Cross Switzerland, Top Ten Countries Turning the Corner on Toxic Pollution 2014. Available at: http://worstpolluted.org/docs/TopTen2014.pdf (Accessed 14 June 2018).

[17] D. Cervantes, R. Sapnu, 20 Bulacan gold smelters shut down (2000). Available at: https://www.philstar.com/nation/2000/10/15/105596/20-bulacan-gold-smelters-shut-down (Accessed 15 June 2018).

[18] Department of Environment and Natural Resources, Water Quality Guidelines and General Effluent Standards of 2016, administrative order 2016–08 (2016). Available at: http://server2.denr.gov.ph/uploads/rmdd/dao-2016–08.pdf (Accessed 07 June 2018).

[19] U.S. Environmental Protection Agency, Guidance Manual for Electroplating and Metal Finishing Pretreatment Standards (1984). Available at: https://www.epa.gov/sites/production/files/ 2015–10/documents/electroplating-and-metal_finishing_pretreatment-guidance_feb-1984.pdf (Accessed 23 May 2018).

[20] Z. Zeledón-Toruño, C. Lao-Luque, M. Solé-Sardans, Nickel and copper removal from aqueous solution by an immature coal (leonardite): effect of pH, contact time and water hardness, J. Chem. Technol. Biotechnol., 80 (2005) 649–656.

[21] M.R. Awual, M. Ismael, T. Yaita, S.A. El-Safty, H. Shiwaku, Y. Okamoto, S. Suzuki, Trace copper(II) ions detection and removal from water using novel ligand modified composite adsorbent, Chem. Eng. J., 222 (2013) 67–76.

[22] S. Taimur, M.I. Hassan, T. Yasin, Removal of copper using novel amidoxime based chelating nanohybrid adsorbent, Eur. Polym. J., 95 (2017) 93–104.

[23] S.S. Rikame, A.A. Mungray, A.K. Mungray, Synthesis, characterization and application of phosphorylated fullerene/sulfonated polyvinyl alcohol (PFSP) composite cation exchange membrane for copper removal, Sep. Purif. Technol., 177 (2017) 29–39.

[24] R.N. Ntimbani, G.S. Simate, S. Ndlovu, Removal of copper ions from dilute synthetic solution using staple ion exchange fibres: dynamic studies, J. Environ. Chem. Eng., 4 (2016) 3143–3150.

[25] Y.-H. Chen, F.-A. Li, Kinetic study on removal of copper(II) using goethite and hematite nano-photocatalysts, J. Colloid Interface. Sci., 347 (2010) 277–281.

[26] N. Aman, T. Mishra, J. Hait, R.K. Jana, Simultaneous photoreductive removal of copper(II) and selenium(IV) under visible light over spherical binary oxide photocatalyst, J. Hazard. Mater., 186 (2011) 360–366.

[27] D. Kanakaraju, S. Ravichandar, Y.C. Lim, Combined effects of adsorption and photocatalysis by hybrid TiO_2/ZnO-calcium alginate beads for the removal of copper, J. Environ. Sci., 55 (2017) 214–223.

[28] C. Liu, X. Lei, L. Wang, J. Jia, X. Liang, X. Zhao, H. Zhu, Investigation on the removal performances of heavy metal ions with the layer-by-layer assembled forward osmosis membranes, Chem. Eng. J., 327 (2017) 60–70.

[29] X. Zhao, C. Liu, Efficient removal of heavy metal ions based on the optimized dissolution-diffusion-flow forward osmosis process, Chem. Eng. J., 334 (2018) 1128–1134.

[30] G. Issabayeva, M.K. Aroua, N.M. Sulaiman, Electrodeposition of copper and lead on palm shell activated carbon in a flow-through electrolytic cell, Desalination, 194 (2006) 192–201.

[31] H.-C. Tao, M. Liang, W. Li, L.-J. Zhang, J.-R. Ni, W.-M. Wu, Removal of copper from aqueous solution by electrodeposition in cathode chamber of microbial fuel cell, J. Hazard. Mater., 189 (2011) 186–192.

[32] A. Lambert, P. Drogui, R. Daghrir, F. Zaviska, M. Benzaazoua, Removal of copper in leachate from mining residues using electrochemical technology, J. Environ. Manage., 133 (2014) 78–85.

[33] G.A. Tonini, L.A.M. Ruotolo, Heavy metal removal from simulated wastewater using electrochemical technology: optimization of copper electrodeposition in a membraneless fluidized bed electrode, Clean. Technol. Envir., 19 (2017) 403–415.

[34] D. Pletcher, F.C. Walsh, Industrial Electrochemistry 2nd edition, Glasglow: Blackie Academic & Professional, 1993.

[35] Caustic soda flakes/Lye/Sodium hydroxide market price (2018). Available at: https://www.mybenta.com/classified/369277/caustic-soda-flakes%2C-lye%2C-sodium-hydroxide%2C-naoh-muntinlupa (Accessed 18 May 2018).

[36] XE Currency Charts: USD to PHP (2018). Available at: https://www.xe.com/currencycharts/?from=USD&to=PHP&view=2YAuthor links open overlay panel (Accessed 18 May 2018).

[37] J.B. Lagare, Power rates up by P0.97/kWh in March – The Manila Times Online (2018). Available at: http://www.manilatimes.net/power-rates-up-by-p0–97-kwh-in-march/385044/ (Accessed 18 May 2018).

[38] D.M. Ayres, A.P. Davis, P.M. Gietka, Removing heavy metals from wastewater, University of Maryland, Engineering Research Center Report, (1994). Available at: http://www.appliedmechtech.com/wp-content/uploads/2016/08/Metal-Precip-Explained-University-of-Maryland.pdf (Accessed 07 May 2018).

[39] Porex Filtration Group, Heavy metal removal from wastewater by precipitation and microfiltration, Available at: http://www.porexfiltration.com/learning-center/technology/precipitation-microfiltration/ (Accessed 07 May 2018).

[40] M. Sillanpää, M. Shestakova, Electrochemical Water Treatment Methods: Fundamentals, Methods and Full Scale Applications, Butterworth-Heinemann, Elsevier Inc., 2017.

[41] M. Paunovic, M. Schlesinger, Fundamentals of Electrochemical Deposition 2nd edition, Wiley-Interscience, John Wiley & Sons, Inc., 2006.

[42] C.G. Zoski, Handbook of Electrochemistry 1st edition, Elsevier B.V., 2007.

[43] S.S. Zumdahl, S.A. Zumdahl, Chemistry 9th edition, Brooks Cole, Cengage Learning, 2014.